

THE SEMIANNUAL REPORT OF THE MSU GROUP

(Jul.-Dec. 1998)

Contributors: V.B.Braginsky (P.I.), I.A.Bilenko, M.L.Gorodetsky,
F.Ya.Khalili, V.P.Mitrofanov, K.V.Tokmakov, S.P.Vyatchanin,
Collaboration with the theoretical group of prof. K.S.Thorne

I. SUMMARY

A. Quantum limits of the sensitivity in the gravitational wave antennae on free masses and intracavity readout meters (M.Gorodetsky, F.Khalili)

The universal formula for the minimal required energy in optical resonators of the antennae attaining resolution at the level of the standard quantum limit is obtained (see Appendix A).

The complete analysis of a new topology of interferometric gravitational wave antenna is presented. This new scheme is based on principles of quantum intracavity measurements of crossquadrature observable and utilizes features of specific quantum state – symphotonic state. It is shown that this scheme can provide the same sensitivity as traditional topologies but at significantly lower levels of circulating power. If characteristic frequency of the gravitational signal is equal to $10^3/2\pi Hz$ then the optical energy stored in the resonators has to be 10^6 erg for the parameters of LIGO, that is 3 orders of magnitude lower than the energy required in traditional schemes if the sensitivity has to be close to the SQL.

In optical bars scheme, intracavity quantum measurement allows to obtain better resolution (better than SQL) with moderate requirements to circulating power.

The key element of the suggested intracavity scheme of gravitational wave antenna is mechanical quantum limited sensor. Currently we are analysing in collaboration with K.Thorne and his group a practical scheme of mechanical QND speed meter.

B. The effect of individual microdust particles in LIGO antenna tubes

(M.Gorodetsky)

Microdust particles inside the tubes of LIGO interferometers may simulate gravitational signal (see Appendix B). Scattering on these particles leads to the shift of resonance frequencies and hence additional phaseshifts between the arms of interferometers. It is shown that even one particle falling from the ceiling of the tube through the beam of interferometer may produce 30ms pulse in output signal with amplitude in dimensionless units $\sim 3 \times 10^{-21}$ for a particle with radius $0.3\mu m$ and $\sim 3 \times 10^{-19}$ for a particle with radius $3\mu m$.

C. The improvement of the Q -factors of the suspensions' modes and the search of the damping effect due to the electric field

**(V.Mitrofanov, N.Styazhkina,
K.Tokmakov)**

The new vacuum chamber (where the tests of the pendulum and violin Qs are performed) was isolated from the rest of the room by a special box which permitted to reduce the level of the contamination of the fiber surface by dust approximately by one order. This box (which is supplied with the special dust free ventilation) also allows to fabricate the fibers for the suspension and to make the welding in the dust free environment as well as to install the pendulum in the chamber within few hours after the fabrication of the fibers. Two pendulums were fabricated during this half of year. Testing of the second one is now in progress. The preliminary result for this pendulum which is a 2-kg fused silica cylinder suspended by two welded fused silica fibers is the following: the quality factor of the torsional-pendulum mode is about 1.4×10^8 . The investigation of the weak dissipation mechanisms at this level of losses is now the main goal of the current researches.

The group continued the study of the electric field damping of the test mass pendulum mode. They have found that the usage of electrodes covered by a gold film in order to applied the electric field creating the control force allows to decrease the field induced losses

more than one order in comparison with aluminium cover. This result has to be regarded as a preliminary one (see details in Appendix C).

**D. Excess noise and thermal noise in the elements of the antenna (I.A.Bilenko,
S.P.Vyatchanin)**

During last six month the method of excess noise measurement in the fused silica mirror suspension was under development. The presence of excess noise in the well stressed metal wire suspension has been proved recently (see the previous annual report). However, it is necessary to obtain a displacement sensitivity approximately 100 times better in order to resolve a thermal fluctuation during the short time intervals as compared to the relaxation time on the fused silica threads, because the quality factor of these threads is about 10^8 against 10^4 for the metal ones. The necessity of preparation and keeping of high quality factor during the measurement is an additional problem. In order to obey the requirements the transducer head placed right on the test mass prototype is designed. The numerical analyses and experimental testing of various transducers are in progress now. For example, the optical displacement sensor based on twin balls whispering-gallery microresonators allows one to reach the sufficient sensitivity of $10^{-13} \text{ cm}/\sqrt{\text{Hz}}$, but its application to the measurement of thread oscillation amplitude meets a number of technique and principal difficulties.

At the same period the distribution of equilibrium thermal fluctuations inside the antenna mirrors was analysed. This analyses shows a principal possibility to extract a contribution of these fluctuations from the antenna output signal. We are planning to finish this analyses soon and obtain the gain parameter and correspondingly the reduction of the requirements to the quality factors of mirrors internal modes.

II. APPENDIX

A. Quantum limits and symphotonic states in free-mass gravitational-wave antennae (B.Braginsky, M.L.Gorodetsky, F.Ya.Khalili)

1. Introduction

In [1,2], we presented an analysis of two qualitatively new schemes for the extraction of information from free-mass gravitational-wave antennas [3]. Common features of these schemes are the use of nonclassical quantum states of the optical field inside the resonators and of QND methods for intracavity measurements of the variations of these states. This becomes possible only with the realization of optical field relaxation times τ_o^* much longer than the measurement time $\tau_{meas} \simeq 10^{-2} \div 10^{-3} s$. One significant advantage of intracavity measurements is that they require lower levels of circulating power than traditional schemes with an antenna with a coherent pump. In [1] and in the subsequent article by Levin [4], the optical cubic nonlinearity $\chi^{(3)}$ of thin plates inserted in an antenna was exploited.

The idea of our second scheme [2], which, in our opinion, can be implemented relatively easily, was to place an additional partially transparent mirror–probe mass at the intersection of the two arms of a gravitational antenna. This results in the formation of two coupled Fabry-Perot resonators. Displacement of the end mirrors under the action of a gravitational wave leads to a redistribution of the energies in the arms, which pushes the central mass. The absolute displacement under optimal conditions is simply equal to the relative displacements of the end mirrors ($hL/2$, where L is the arm length and h is the amplitude of the variation of the metric), and the light in the system behaves like a rigid bar. The displacement associated with an independent mass that does not interact with the optical field can be registered without consuming a large amount of power. A rigorous general relativistic justification of the schemes in [1,2] can be found in [5].

The merits of this intracavity measurement are the following: a) in the resonators, the required nonclassical quantum state (close to a Fock state) is formed automatically; b) direct

measurement of a displacement $hL/2$ consumes relatively little power; c) precision higher than the standard quantum limit can be obtained.

In [2], we did not make an analysis of the minimal energy of the optical field \mathcal{E} in the system required to preserve the sensitivity. Another important unanalysed problem is the connection between the achievable resolution and a chosen procedure for displacement measurement.

It is important to note here that the provision of substantial values of \mathcal{E} is a key problem for large-scale gravitational wave antennas, and that this problem has not a technical but a fundamental nature. Indeed, the proposed sensitivity levels of such antennas will be close to the standard quantum limit for the displacement of the masses M of the end mirrors:

$$\Delta x_{SQL}(M) = Lh_{SQL} \simeq \sqrt{\frac{\hbar}{M\omega_{gr}^2\tau_{gr}}}, \quad (1)$$

where ω_{gr} is the frequency of the gravitational signal and τ_{gr} is its duration (we omit in our estimates numerical terms of the order of unity that depend on the form of the signal). According to the Heisenberg uncertainty relation, the momentum should be perturbed by a value of the order of:

$$\Delta p = \frac{\hbar}{2\Delta x_{SQL}} \simeq \sqrt{\hbar M\omega_{gr}^2\tau_{gr}} \quad (2)$$

This perturbation must be provided by the uncertainty in the energy \mathcal{E} in the interferometer, which, thus, cannot be less than

$$\Delta\mathcal{E} = \sqrt{\frac{\omega_{gr}}{\tau_{gr}}}L\Delta p = L\sqrt{\hbar M\omega_{gr}^3} \quad (3)$$

This value is not especially large; for example, for $L = 4 \times 10^5 \text{ cm}$, $\omega_{gr} = 10^3 \text{ s}^{-1}$, and $M = 10^4 \text{ g}$ (the parameters of the LIGO antenna),

$$\Delta\mathcal{E} \simeq 4 \times 10^{-2} \text{ erg}, \quad (4)$$

and in the case of nonclassical states of the optical field, in which $\Delta\mathcal{E} \sim \mathcal{E}$, the necessary resolution can be obtained at very low energies. However, for coherent states in which

$$\Delta\mathcal{E} = \sqrt{\hbar\omega_o\mathcal{E}}, \quad (5)$$

where ω_o is the optical frequency, the requirements are very strict:

$$\mathcal{E} \simeq \frac{ML^2\omega_{gr}^3}{\omega_o}. \quad (6)$$

For the same parameters as before and $\omega_o = 2 \times 10^{15} s^{-1}$,

$$\mathcal{E}_{SQL} \simeq 10^9 erg, \quad (7)$$

and if $\omega_{gr} = 10^4 s^{-1}$, then

$$\mathcal{E}_{SQL} \simeq 10^{12} erg. \quad (8)$$

In this paper, we analyze a new intracavity scheme that is, in some sense, complementary to the ‘‘optical bars’’ scheme. In this scheme, the optical field forms in a quantum state that is close to states with squeezed phase; this is known to allow, in principle, a dramatic decrease in the optical quanta because $\delta\varphi \sim 1/N$. (Non-QND measurement of a similar observable was proposed in [6]).

2. A crossquadrature quantum observable and a scheme for its measurement

The basic idea of the new scheme for an intracavity readout system is the use of two modes excited in the Fabry-Perot resonators of the antenna’s orthogonal arms. If the modes are not linearly coupled (this is critical in this scheme), they can be tuned as close to each other as $(\omega_1 - \omega_2)\tau_{meas} \ll 1$. As a result, the frequency variation in one (or both) resonators produced by a gravitational wave will lead to the appearance of a phase difference with the oscillation amplitude

$$\delta\varphi \simeq \frac{\hbar\omega_o}{\omega_{gr}}, \quad (9)$$

which we propose to register. Since no meter has been invented thus far to directly register the phase difference between two quantum electromagnetic oscillators, another variable proportional to $\delta\varphi$ is required.

We propose to measure the averaged product of the two quadrature components of two different oscillators, which, in the limit of large numbers of quanta, is very close to a phase measurement. One possible scheme for the realization of the proposed crossquadrature observable is depicted in Fig.1. This scheme is based on the use of ponderomotive nonlinearity in a way similar to that in [2]. Mirrors A' and B' direct the optical beams reflected from the end mirrors A and B and transmitted by the 50% beamsplitter C on opposite sides of the double highly reflecting (zero transmission) mirror D (to eliminate linear coupling). In the engineering realization of this scheme, A' and B' can be rigidly connected to the beamsplitter, and can be focusing reflectors, making it possible for the mass m of D to be smaller.

It is easy to see that, due to the beamsplitter, the optical beams from arms A–C and B–C interfere in the shorter arms such that one of them has amplitude proportional to $a_1 + ia_2$ and the other has amplitude proportional to $a_2 + ia_1$ ($a_{1,2}$ are the complex field amplitudes in the longer arms). This is valid if the geometrical conditions in Fig.1 are satisfied. As a result, the ponderomotive force F_{pond} acting on mirror D will be proportional to:

$$F_{pond} \propto |a_1 + ia_2|^2 - |a_2 + ia_1|^2 \simeq 4|a_1||a_2|\delta\varphi. \quad (10)$$

Provided that the initial optical energy $\mathcal{E}/2$ in the two arms is nearly the same ($\mathcal{E} = \hbar\omega_o N = \hbar\omega_o a^2$, $a = |a_1| = |a_2|$), in a quasistatic approximation, this force will be

$$F_{pond} \simeq \frac{\mathcal{E}}{L}\delta\varphi \quad (11)$$

Note here that there is no direct linear coupling between modes in this scheme. In other words, modes in the resonator are coupled via the $\chi^{(3)}$ nonlinearity resulting from the ponderomotive effect. Linear coupling is due only to the movement of the mirror D . The shift of D changes the lengths of the shorter arms, changing the interference conditions on the beamsplitter, which consequently leads to a redistribution of the optical photons between the two modes.

This scheme realizes indirect QND measurement of the operator

$$\hat{\mathcal{X}}_{\pi/2} = i(\hat{a}_1^+ \hat{a}_2 - \hat{a}_2^+ \hat{a}_1), \quad (12)$$

where $\hat{a}_{1,2}^+$ and $\hat{a}_{1,2}$ are the creation and annihilation operators for two different oscillators with the same frequencies ω . The operator $\hat{\mathcal{X}}_{\pi/2}$ presents a special case of the family of operators

$$\hat{\mathcal{X}}_{\theta} = \hat{a}_1^+ \hat{a}_2 e^{i\theta} + \hat{a}_2^+ \hat{a}_1 e^{-i\theta}, \quad (13)$$

which we propose to name crossquadrature operators. These operators commute with the Hamiltonian of the two modes:

$$[\hat{\mathcal{X}}_{\theta}, \hbar\omega(\hat{a}_1^+ \hat{a}_1 + \hat{a}_2^+ \hat{a}_2)] = 0, \quad (14)$$

i.e., they are, indeed, QND variables. The eigenstates of the crossquadrature operators have the form

$$|N, n\rangle = \frac{1}{\sqrt{2^N n!(N-n)!}} (\hat{a}_1^+ + \hat{a}_2^+ e^{-i\theta})^n (\hat{a}_1 + \hat{a}_2 e^{i\theta})^{N-n} |0\rangle, \quad (15)$$

where N is the sum of quanta in the system and n is an integer in the range from 0 to N . In this state, each of the N quanta has equal probability to reside in either arm of the interferometer. However, the amplitudes of these probabilities for n quanta are orthogonal to those of the other $N - n$ quanta. Due to this peculiar entanglement between the modes, we shall call eigenstates of the crossquadrature operator symphotonic quantum states.

The eigenvalues of the operator $\hat{\mathcal{X}}_{\theta}$ are $n - (N - n) = 2n - N$, i.e., measuring the crossquadrature variable, the observer determines the difference between the two kinds of quanta. Symphotonic states (15) are very sensitive to the change of the phase difference in the two oscillators. As we show in Appendix A, a phase shift leads to a transition between states with different n (preserving the total number of quanta), that can be detected by measuring $\hat{\mathcal{X}}_{\pi/2}$. The probability of this transition is equal in the case $\delta\varphi \ll 1$ to

$$p = \frac{\delta\varphi^2}{4}(N + 2n(N - n)), \quad (16)$$

and when $n \simeq N/2$, p tends to unity when $\delta\varphi \simeq \sqrt{8}/N$, thus allowing, in principle, the registration of these small phase shifts.

3. Limitations on the sensitivity

It is not difficult to show that the finite masses of the mirrors A' and B' , as well as the mass of the beamsplitter C , do not influence the behavior of the system if these masses are substantially greater than the mass m . We will use a standard linear approximation, in which the optical field can be represented as the sum of the large classical dimensionless amplitude \mathcal{A} and the quantum annihilation operator \hat{a} , neglecting terms of the order of \hat{a}^2 and higher. We suppose also that τ_o^* and relaxation time τ_m^* of the mass m is very large in comparison with other characteristic times. In this case, the equations of motion will have the form:

$$\begin{aligned}
\frac{d\hat{a}_1(t)}{dt} &= \omega_o \mathcal{A} \left(\frac{i\hat{x}_1(t) - \hat{x}(t)}{L} + \frac{ih(t)}{2} \right) + \int_0^\infty \sqrt{\frac{\delta_o}{\pi}} \hat{b}_1(\omega) e^{-i(\omega+\omega_o)t} d\omega \\
\frac{d\hat{a}_2(t)}{dt} &= \omega_o \mathcal{A} \left(\frac{i\hat{x}_2(t) + \hat{x}(t)}{L} - \frac{ih(t)}{2} \right) + \int_0^\infty \sqrt{\frac{\delta_o}{\pi}} \hat{b}_2(\omega) e^{-i(\omega+\omega_o)t} d\omega \\
m \frac{d^2\hat{x}(t)}{dt^2} &= \frac{i\hbar\omega_o \mathcal{A}}{L} (\hat{a}_1^+(t) - \hat{a}_1(t) + \hat{a}_2(t) - \hat{a}_2^+(t)) + \hat{F}^{meter}(t) + \hat{F}^{mech}(t) \\
M \frac{d^2\hat{x}_1(t)}{dt^2} &= \frac{\hbar\omega_o \mathcal{A}}{L} (\hat{a}_1(t) + \hat{a}_1^+(t)) \\
M \frac{d^2\hat{x}_2(t)}{dt^2} &= \frac{\hbar\omega_o \mathcal{A}}{L} (\hat{a}_2(t) + \hat{a}_2^+(t))
\end{aligned} \tag{17}$$

where $x_{1,2}$ are the displacements of the mirrors A and B , x is the displacement of D , $\delta_o = 1/2\tau_o^*$ is the decrement of the optical losses in the resonators, $\hat{b}_{1,2}(\omega)$ are the corresponding annihilation operators for the heatbath modes, which satisfy the commutational relations

$$[\hat{b}_{1,2}(\omega), \hat{b}_{1,2}^+(\omega')] = \delta(\omega - \omega'), \tag{18}$$

F^{meter} is the fluctuational reaction of the coordinate meter on the mirror D with mass m , $h(t)/2$ is the relative change of the optical lengths of the resonators (in the case of a gravitational antenna, this is the dimensionless metric variation), and F^{mech} is the Nyquist fluctuational force acting on the mass m .

The characteristic equation of this system is:

$$p^6 + \nu^6 = 0, \tag{19}$$

where

$$\nu = \left(\frac{2\omega_o^2 \mathcal{E}^2}{mML^4} \right)^{1/6}. \quad (20)$$

It has roots with positive real parts of the order of ν . Thus, there exists in the system a dynamic instability with a characteristic time ν^{-1} . To suppress this with a feedback loop, it is necessary to have

$$\nu < \omega_{gr}. \quad (21)$$

The signal-to-noise ratio is equal to (see Appendix B):

$$\frac{s}{n} = \frac{\omega_o^2 \mathcal{E}^2}{L^2} \int_{-\infty}^{\infty} \frac{\omega^6 |h_\omega(\omega)|^2}{m^2(\nu^6 - \omega^6)^2 S_x + 2m\omega^4(\nu^6 - \omega^6) S_{xF} + \omega^8(S_F + S_m + S_o)} \frac{d\omega}{2\pi}, \quad (22)$$

where $h_\omega(\omega)$ is the signal spectrum,

$$S_m = \frac{2\kappa T m}{\tau_m^*} \quad (23)$$

is the spectral density of F^{mech} (κ is the Boltzmann constant and T is the temperature),

$$S_o = \frac{\hbar \omega_o \mathcal{E}}{L^2 \tau_o^* \omega^2} \quad (24)$$

is the spectral density of the fluctuational force due to dissipation in the optical resonators, S_x and S_F are the spectral densities of the additive noise x^{meter} of the meter and of F^{meter} , and S_{xF} is the cross spectral density of x^{meter} and F^{meter} . The values of S_F , S_x and $S_{xF}(\omega)$ must obey the Heisenberg inequality [7]:

$$S_x(\omega) S_F(\omega) - S_{xF}^2(\omega) \geq \frac{\hbar^2}{4}. \quad (25)$$

The condition for the detection of a signal can be represented in the form:

$$h \geq \sqrt{h_{meter}^2 + h_{mech}^2 + h_{opt}^2}, \quad (26)$$

where

$$h_{mech} = \frac{L\omega_{gr}}{\mathcal{E}\omega_o} \sqrt{\frac{2\kappa T m}{\tau_m^* \tau_{gr}}} = 2 \frac{\omega_{gr}}{\nu^3} \sqrt{\frac{2\kappa T}{\tau_m^* \tau_{gr} M}} \quad (27)$$

is the limit due to the thermal noise of the mass m ,

$$h_{opt} = \sqrt{\frac{1}{\omega_o^2 \tau_o^* \tau_{gr} N}} \quad (28)$$

is the limit due to the optical losses (τ_{gr} is the duration of the signal), and h_{meter} is the limit due to the quantum noise of the meter.

It is important to note that the limitation (28) is also valid for the previous scheme [2], based on a different principle for intracavity measurement (this follows from formula (10) of [2]).

The value of h_{meter} is determined by the magnitudes of the spectral densities $S_x(\omega)$, $S_F(\omega)$, and $S_{xF}(\omega)$ and their frequency dependence. In the case of a plain coordinate meter:

$$S_x(\omega) = \text{const}, \quad S_F(\omega) = \text{const}, \quad S_{xF}(\omega) = 0. \quad (29)$$

With regard to limitation (21), values corresponding to optimal tuning of the meter will be:

$$S_F = \frac{\hbar m \omega_{gr}^2}{2}, \quad S_x = \frac{\hbar}{2m \omega_{gr}^2}. \quad (30)$$

The ultimate sensitivity of the meter is determined, in this case, by the formula

$$h_{meter} = \frac{L}{\omega_o \mathcal{E}} \sqrt{\frac{\hbar m \omega_{gr}^4}{\tau_{gr}}} = \sqrt{2} \left(\frac{\omega_{gr}}{\nu} \right)^3 h_{SQL}(M). \quad (31)$$

Thus, because of (21), it is impossible in this case to reach a sensitivity corresponding to $h_{SQL}(M)$.

To preserve a sensitivity at the level of $h_{SQL}(M)$ and lower the requirements on the energy, one can use an advanced meter providing higher precision for monitoring the mass m . A speed meter [9] can be used for this monitoring. This can be realized in the form of an ordinary parametric electromagnetic displacement transducer (operating at microwave wavelengths) with an additional buffering cavity, coupled with the main (working) cavity [9]. We show in Appendix C that, in this case,

$$S_x(\omega) = \frac{\hbar d^2 \Omega_e^4}{4\omega^2 \omega_e W_e \sin^2 \Phi}, \quad S_F(\omega) = \frac{\hbar \omega_e W_e \omega^2}{d^2 \Omega_e^4}, \quad S_{xF}(\omega) = -\frac{\hbar}{2} \cot \Phi, \quad (32)$$

where ω_e is the microwave frequency, W_e is the microwave pump power, d is an equivalent parameter with the dimensions of length, which characterizes the tunability of the transducer [10]:

$$d^{-1} = \frac{1}{\omega_e} \frac{\partial \omega_e}{\partial x}, \quad (33)$$

Ω_e is the beat frequency between the working and buffering resonators, which must satisfy the conditions $\Omega_e \gg \omega_{gr}$ and $\Omega_e/\tau_e^* \gg \omega_{gr}^2$ (τ_e^* is the relaxation time due to the coupling with the transmission line), and Φ is the phase of the local oscillator used for detection of the microwave signal. For optimal tuning of the meter parameters, when

$$W_e = \frac{m d^2 \Omega_e^4 \omega_{gr}^6}{2\omega_e \nu^6} \quad (34)$$

and

$$\cot \Phi = -\frac{\omega_{gr}^6}{\nu^6}, \quad (35)$$

the limiting sensitivity will be

$$h_{meter} = \sqrt{2} h_{SQL}(M). \quad (36)$$

If, for example, $\omega_o = 2 \times 10^{15} s^{-1}$, $L = 4 \times 10^5 cm$, $\omega_{gr} = 10^3 s^{-1}$ (these values correspond to the values for the LIGO antenna [3]), $m = 1g$, and $\mathcal{E} = 10^6 erg$, then $\nu \simeq 5 \times 10^2 s^{-1}$, and condition (21) is satisfied. If in addition $d = 1cm$ (the value achieved in high-Q sapphire disk resonators [11]) and $\Omega_e = 3 \times 10^3 s^{-1}$, then the required microwave pump power will be $W_e = 3 \times 10^4 erg/s$. Thus, the analyzed scheme makes it possible to dramatically decrease the requirements for the optical circulating energy by using a microwave transducer with a reasonable set of parameters.

Under these conditions, however, the requirements for the level of dissipation in the probe mass m increase as the signal that must be registered decreases:

$$\Delta v_m \simeq \frac{\nu^3}{\omega_{gr}^3} \Delta v_{SQL}, \quad (37)$$

where

$$\Delta v_{SQL} = \sqrt{\frac{\hbar}{m\tau_{gr}}} \quad (38)$$

If the above parameters are chosen, $\Delta v_m \simeq 1/8\Delta v_{SQL}$. In order for the dissipation not to deteriorate the sensitivity, it is necessary that $h_{mech} < h_{meter}$, or

$$\frac{2\kappa T}{\tau_m^*} < \frac{\hbar\nu^6}{4\omega_{gr}^4}. \quad (39)$$

For example, for $T = 4K$, $\tau_m^* > 3 \times 10^8 s$. Thus, the requirements for the dissipation in the mass m are severe, but achievable [12].

Losses in the optical resonator will not influence the sensitivity if $h_{opt} < h_{meter}$, which is equivalent to the condition

$$\tau_o^* > \frac{\mathcal{E}_{SQL}}{\mathcal{E}\omega_{gr}}, \quad (40)$$

or, for the parameter values introduced above, $\tau_o^* > 1s$. This is quite possible in a LIGO-type detector with optical mirrors available today.

4. Comparison with the “optical bar” scheme

In [2], not all regimes for the “optical bar” scheme were analyzed in detail. Moreover, there was unfortunately an error in the formula following formula (12) (term “1” under the root should be omitted).

Here, we shall limit our treatment to “wideband” regimes, when the range of the signal frequencies is far from the resonant frequencies in the signal-to-noise integral; these regimes are the most useful from the practical point of view. The “narrowband” regime, in which it is possible to attain sensitivity better than the SQL, has already been considered in detail in [2]. In our analysis, we shall assume that $\omega_{gr} < \Omega$ (Ω is the beat frequency in the system of two coupled optical resonators; the case of $\omega_{gr} > \Omega$ is difficult to realize in practice, and

does not provide any interesting new results) and $m \ll M$. The behavior of the system is determined by the parameter with the dimensions of frequency

$$\Theta = \left(\frac{2\omega_o \mathcal{E} \Omega}{L^2} \left(\frac{1}{m} + \frac{1}{2M} \right) \right)^{1/4} \quad (41)$$

This frequency describes the influence of the ponderomotive force on the dynamics of the system, and plays a role analogous to ν (see formula (20)).

It is possible to distinguish three cases, depending on the level of the circulating energy (the value of Θ).

5. *Weak pump power, $\Theta^2 < \omega_{gr}\Omega$*

If a plain coordinate meter is used, the calculations give the following result:

$$h_{meter} = \left(\frac{\omega_{gr}\Omega}{\Theta^2} \right)^2 h_{SQL}(m) > h_{SQL}(m), \quad (42)$$

where

$$h_{SQL}(m) = \frac{1}{L} \sqrt{\frac{\hbar}{m\omega_{gr}^2\tau_{gr}}} \quad (43)$$

If a speed meter is used, the sensitivity can be higher:

$$h_{meter} = \frac{\omega_{gr}\Omega}{\Theta^2} h_{SQL}(m) > h_{SQL}(m), \quad (44)$$

but is still lower than even $h_{SQL}(m)$.

Intermediate case, $\omega_{gr}\Omega < \Theta^2 < \omega_{gr}\Omega\sqrt{2M/m}$

For a plain coordinate sensor, the best sensitivity in this case is

$$h_{meter} = \frac{\omega_{gr}\Omega}{\Theta^2} h_{SQL}(m), \quad (45)$$

i.e., h_{meter} is smaller than $h_{SQL}(m)$, and $h_{meter} \rightarrow h_{SQL}(M)$ if $\Theta^2 \rightarrow \omega_{gr}\Omega\sqrt{2M/m}$. The required optical energy in this case is

$$\mathcal{E} = \frac{\Omega}{\omega_{gr}} \mathcal{E}_{SQL} > \mathcal{E}_{SQL}. \quad (46)$$

The use of a speed meter in this regime does not give a gain in sensitivity, however an increase in sensitivity is possible if an advanced coordinate detector with correlated noises is used ($S_{xF} \neq 0$) [8]. In this case

$$h_{meter} = \left(\frac{\omega_{gr}\Omega}{\Theta^2} \right)^2 h_{SQL}(m), \quad (47)$$

if $\Theta^2 < \omega_{gr}\Omega\sqrt{2M/m}$, and

$$h_{meter} = h_{SQL}(M) \quad (48)$$

otherwise. The required energy in the latter case can be lower than \mathcal{E}_{SQL} , but with respect to a possible dynamical instability, which appears when $\Theta^2 \geq \Omega^2/4$:

$$\mathcal{E} > \sqrt[8]{\frac{8m}{M}} \mathcal{E}_{SQL} \quad (49)$$

Strong pump power, $\Theta^2 \gg \omega_{gr}\Omega\sqrt{2M/m}$

This is the ‘‘optical bar’’ regime, when the masses M and m move together, and are connected by electromagnetic rigidity. In this case, a plain coordinate meter provides a sensitivity corresponding to the standard quantum limit $h_{SQL}(M)$, and use of a speed meter makes it possible to overcome this limit, but with higher energy:

$$h_{meter} = \frac{\omega_{gr}\Omega}{\Theta^2} h_{SQL}(m) = \sqrt{\frac{\mathcal{E}_{SQL}\Omega}{\mathcal{E}\omega_{gr}}} h_{SQL}(M) \quad (50)$$

Note that, in this case, also, the total mass $\sim 2M$ is present in the expression for the thermal limit. This result is quite understandable, since, in this regime, thermal fluctuations of the small mass m act on the large compound mass $2M + m$.

6. Conclusion

Quantum mechanics sets severe limits on the sensitivity and the required circulating energy in traditional free-mass gravitational-wave antennas. One possible way to beat these

limits is to use intracavity QND measurements. In this paper, we have analyzed a new QND observable and its corresponding symphotonic quantum states, which possess a number of features that make it promising for experiments requiring registration of small phase variations:

1) Unlike other known QND observables, this one is a joint integral of motion for two quantum oscillators with equal frequencies.

2) The crossquadrature observable is very sensitive to the phase difference of the oscillators. Phase differences of the order of $1/N$ (the theoretical limit for phase measurements) can be detected, where N is number of quanta in the system.

3) Well-known methods for the QND measurement of electromagnetic energy can be used to measure this new observable.

We have considered a practical optical scheme in which the new observable can be used for the detection of gravitational waves. Our estimates show that, in combination with advanced coordinate meters, this scheme provides a sensitivity of the same order as that for planned antennas at significantly lower energies.

Summarizing the results of this article and of [1,2,4], we conclude that intracavity measurements with automatically organizing nonclassical optical quantum states make it possible, in principle, to lower the required power levels and in several cases to achieve sensitivity better than the standard quantum limit.

We note also that the schemes we have analyzed do not cover all possible geometries for intracavity measurements with ponderomotive nonlinearity. Better realizations with higher responses are probably possible.

7. appendix

a. The evolution of a symphotonic state

$$\hat{U}(\phi_1, \phi_2) = \exp\left(\frac{\phi_1 \hat{n}_1 + \phi_2 \hat{n}_2}{i\hbar}\right) \quad (51)$$

where $\hat{n}_{1,2}$ are the operators for the number of quanta in the modes. Hence

$$\hat{U}(\phi_1, \phi_2)\hat{a}_1^+\hat{U}^\dagger(\phi_1, \phi_2) = \hat{a}_1^+ e^{-i\phi_1}, \quad (52)$$

$$\hat{U}(\phi_1, \phi_2)\hat{a}_2^+\hat{U}^\dagger(\phi_1, \phi_2) = \hat{a}_2^+ e^{-i\phi_2}, \quad (53)$$

and

$$\hat{U}(\phi_1, \phi_2)|0\rangle = |0\rangle. \quad (54)$$

Taking into account formula (15) and omitting the unimportant factor $e^{-\frac{i(\phi_1+\phi_2)N}{2}}$, we can obtain:

$$\hat{U}(\phi_1, \phi_2)|N, n\rangle = \frac{1}{\sqrt{2^N n!(N-n)!}} (\hat{A}^+ \cos \delta\phi + iB^+ \sin \delta\phi)^n (\hat{B}^+ \cos \delta\phi + iA^+ \sin \delta\phi)^{N-n} |0\rangle \quad (55)$$

where

$$\hat{A}^+ = a_1^+ + a_2^+ e^{-i\theta}, \quad \hat{B}^+ = a_1^+ - a_2^+ e^{-i\theta} \quad (56)$$

and

$$\delta\phi = \phi_2 - \phi_1. \quad (57)$$

If $\delta\phi \ll 1$ then

$$\begin{aligned} \hat{U}(\phi_1, \phi_2)|N, n\rangle &\simeq \left(1 - \frac{\delta\phi^2}{8}(N + 2n(N-n))\right) |N, n\rangle + \\ &i\delta\phi \left(\sqrt{n(N-n+1)}|N, n-1\rangle + \sqrt{(n+1)(N-n)}|N, n+1\rangle\right) - \\ &\frac{\delta\phi^2}{2} \left(\sqrt{n(n-1)(N-n+1)(N-n+2)}|N, n-2\rangle + \right. \\ &\left. \sqrt{(n+1)(n+2)(N-n)(N-n-1)}|N, n+2\rangle\right) \end{aligned} \quad (58)$$

Thus, the probability for changing the number n is equal to

$$p = 1 - |\langle N, n | \hat{U}(\phi_1, \phi_2) | N, n \rangle|^2 \simeq \frac{\delta\phi^2}{4}(N + 2n(N-n)). \quad (59)$$

b. *Signal-to-Noise ratio*

Equations (17) can be rewritten in the form:

$$\begin{aligned}
\frac{d\hat{\mathcal{N}}(t)}{dt} &= -\frac{2\omega_o N}{L}\hat{x}(t) + \mathcal{A} \int_0^\infty \sqrt{\frac{\delta_o}{\pi}} \left((\hat{b}_1^+(\omega) - \hat{b}_2^+(\omega)) e^{i(\omega+\omega_o)t} + h.c. \right) d\omega \\
\frac{d\hat{\mathcal{X}}_{\pi/2}(t)}{dt} &= \frac{2\omega_o N}{L}\hat{y}(t) + \omega_o N h(t) + \mathcal{A} \int_0^\infty i \sqrt{\frac{\delta_o}{\pi}} \left((\hat{b}_1^+(\omega) - \hat{b}_2^+(\omega)) e^{i(\omega+\omega_o)t} + h.c. \right) d\omega \\
m \frac{d^2 x(t)}{dt^2} &= \frac{\hbar\omega_o}{L} \hat{\mathcal{X}}_{\pi/2}(t) + \hat{F}^{meter}(t) \\
2M \frac{d^2 \hat{y}(t)}{dt^2} &= \frac{\hbar\omega_o}{L} \hat{\mathcal{N}}(t)
\end{aligned} \tag{60}$$

where

$$\hat{\mathcal{N}} = \mathcal{A}(\hat{a}_1 + \hat{a}_1^+ - \hat{a}_2 - \hat{a}_2^+), \quad \hat{\mathcal{X}}_{\pi/2} = i\mathcal{A}(\hat{a}_2 - \hat{a}_2^+ - \hat{a}_1 + \hat{a}_1^+), \tag{61}$$

$\hat{\mathcal{N}}$ - difference of number of quanta in the two arms, $y = (x_1 - x_2)/2$, and *h.c.* stands for Hermitian conjugation. Hence, the spectrum of $x(t)$ is equal to

$$x(\omega) = x_{signal}(\omega) + X(\omega), \tag{62}$$

where

$$x_{signal}(\omega) = \frac{\hbar\omega_o^2 N}{mL} \frac{-i\omega^3}{\nu^6 - \omega^6} h(\omega) \tag{63}$$

is the signal spectrum,

$$X(\omega) = \frac{\omega^4}{m(\nu^6 - \omega^6)} \left(F^{meter}(\omega) + F^{mech}(\omega) + F^{opt}(\omega) \right) \tag{64}$$

is the spectrum of fluctuations of $x(t)$, and $F^{opt}(\omega)$ is the spectrum of force

$$F^{opt}(t) = \frac{\hbar\omega_o \mathcal{A}}{L} \int_0^\infty \sqrt{\frac{\delta_{opt}}{\pi}} \left[\left(\frac{1}{i\omega} + \frac{\omega_o \mathcal{E}}{ML^2\omega^4} \right) (\hat{b}_1^+(\omega) - \hat{b}_2^+(\omega)) e^{i(\omega+\omega_o)t} d\omega + h.c. \right] \tag{65}$$

The output signal of the coordinate meter is equal to

$$\tilde{x}(t) = x(t) + x^{meter}(t), \tag{66}$$

where $x^{meter}(t)$ is the additive noise of the meter. Hence,

$$\tilde{x}(\omega) = x(\omega) + x^{meter}(\omega) = x_{signal}(\omega) + X(\omega) + x^{meter}(\omega), \quad (67)$$

and the SNR is equal to (22).

c. Microwave speed meter

Let us consider two coupled microwave resonators. The first is connected to an output waveguide (see Fig.2), and it's eigenfrequency depends on the coordinate x to be measured:

$$\tilde{\omega}(x) = \omega_e \left(1 - \frac{x}{d}\right), \quad (68)$$

while the second is pumped by the resonant power $U_0 \cos \omega_e t$.

The equations of motion for such a system are

$$\begin{aligned} \frac{d^2 q_1(t)}{dt^2} + 2\delta_e \frac{dq_1(t)}{dt} + \omega_e^2 \left(1 - \frac{x(t)}{d}\right)^2 q_1(t) &= 2\omega_e \Omega_e q_2(t) + \frac{2\omega_e}{\rho} U^{fluct}(t) \\ \frac{d^2 q_2(t)}{dt^2} + \omega_e^2 q_2(t) &= 2\omega_e \Omega_e q_1(t) + \frac{\omega_e}{\rho} U_0 \cos \omega_e t, \end{aligned} \quad (69)$$

where $q_{1,2}$ are the generalized coordinates of the resonators, ρ is the wave impedance of the resonators, $\delta_e = 1/2\tau_e^*$, τ_e^* is the relaxation time of loaded first resonator, and U^{fluct} are fluctuations in the waveguide (we neglect intrinsic losses and corresponding fluctuations of the resonators).

Linearizing these equations in the strong-pumping approximation and using the method of slowly varying amplitudes, we can obtain:

$$\begin{aligned} \frac{da_1(t)}{dt} + \delta_e a_1(t) &= -\Omega_e b_2(t) - \frac{U_s^{fluct}(t)}{\rho} \\ \frac{db_1(t)}{dt} + \delta_e b_1(t) &= \frac{\omega_e q_0}{d} x(t) + \Omega_e a_2(t) + \frac{U_c^{fluct}(t)}{\rho} \\ \frac{da_2(t)}{dt} &= -\Omega_e b_1(t) \\ \frac{db_2(t)}{dt} &= \Omega_e a_1(t) \end{aligned} \quad (70)$$

where $a_{1,2}$ and $b_{1,2}$ are the amplitudes of the cosine and sine quadrature components of $q_{1,2}$, $U_{c,s}^{fluct}$ are the same for U^{fluct} , and q_0 is the mean value of the amplitude of oscillations in the first resonator.

Solution of these equations in the spectral representation gives:

$$a_1(\omega) = -\frac{i\omega U_s^{fluct}(\omega)}{\rho \mathcal{L}(\omega)}, \quad b_1(\omega) = \frac{i\omega}{\mathcal{L}(\omega)} \left(\frac{\omega_e q_0}{d} x(\omega) + \frac{U_c^{fluct}(\omega)}{\rho} \right), \quad (71)$$

where $\mathcal{L}(\omega) = \Omega_e^2 - \omega^2 + i\omega\delta_e$. The output wave in the waveguide can be represented in the form:

$$U^{out}(t) = U^{fluct}(t) - \frac{2\delta_e \rho}{\omega_e} \frac{dq_1(t)}{dt} = \\ \left(U_c^{fluct}(t) - 2\delta_e \rho b_1(t) \right) \cos \omega_e t + \left(U_s^{fluct}(t) + 2\delta_e \rho a_1(t) \right) \sin \omega_e t \quad (72)$$

If a homodyne detector with $U_{LO} \propto \sin(\omega_e t + \Phi)$ is used, where Φ is the phase of the local oscillator, the output signal of the detector is proportional to

$$\tilde{U}(t) = \left(U_c^{fluct}(t) - 2\delta_e \rho b_1(t) \right) \sin \Phi + \left(U_s^{fluct}(t) + 2\delta_e \rho a_1(t) \right) \cos \Phi \quad (73)$$

Substitution into this expression of the solution (71) gives that the spectrum of \tilde{U} is equal to

$$\tilde{U}(\omega) = -\frac{2i\omega\omega_e\delta_e\rho q_0 \sin \Phi}{\mathcal{L}(\omega)d} \left(x(\omega) + x^{meter}(\omega) \right), \quad (74)$$

where

$$x^{meter}(\omega) = -\frac{d}{2i\omega\omega_e\delta_e q_0 \rho \sin \Phi} \left(i\omega(\Omega_e^2 - \omega^2 - i\omega\delta_e) \right) \left(U_c^{fluct}(\omega) \sin \Phi + U_s^{fluct}(\omega) \cos \Phi \right) \quad (75)$$

is the spectrum of the additive noise of the meter.

The fluctuational reaction force of the meter is equal to

$$F^{meter}(t) = \frac{q_0 \rho \omega_e}{d} a_1(t), \quad (76)$$

or, in spectral form,

$$F^{meter}(\omega) = -\frac{i\omega\omega_e q_0 U_s^{fluct}(\omega)}{\mathcal{L}(\omega)d} \quad (77)$$

If the frequency ω is relatively small:

$$\omega^2 \ll \Omega_e^2 \quad \text{and} \quad \omega\delta_e \ll \Omega_e^2 \quad (78)$$

then expressions (77,75) directly give the spectral densities (32).

FIGURES

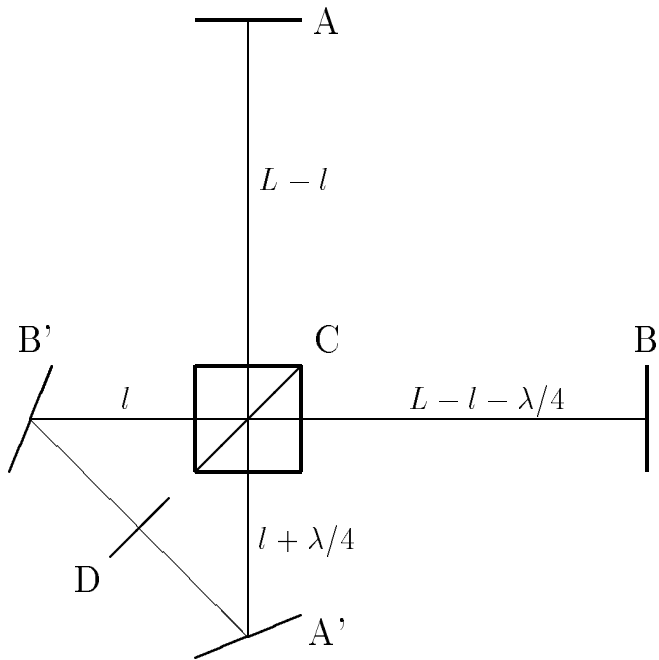


FIG. 1. The scheme of measurement of the crossquadrature observable

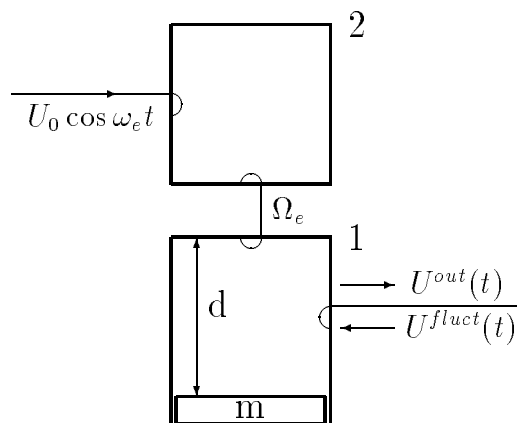


FIG. 2. The scheme of microwave speedmeter

REFERENCES

- [1] V.B.Braginsky, F.Ya.Khalili, Phys. Lett. A **218** (1996) 167
- [2] V.B.Braginsky, M.L.Gorodetsky, F.Ya.Khalili, Phys. Lett. A **232** (1997) 340
- [3] A.Abramovici et al., Science **256** (1992) 325.
- [4] Yu.Levin, Phys.Rev. **D57** (1998) 659.
- [5] M.V.Sazhin, S.N.Markova, Phys. Lett. A **233** (1997) 43.
- [6] M.J.Holland, K.Burnett, Phys. Rev. Lett **71** (1993) 1355.
- [7] V.B.Braginsky, F.Ya.Khalili, "Quantum Measurement", ed. K.S.Thorne, Cambridge Univ. Press, 1992.
- [8] A.V.Syrtsev, F.Ya.Khalili, Zh. Eksp. Teor. Fiz. **106** (1994) 744.
- [9] V.B.Braginsky, F.Ya.Khalili, Phys. Lett. A **147** (1990) 251.
- [10] V.B.Braginsky, M.L.Gorodetsky, V.S.Iltchenko, S.P.Vyatchanin, Phys. Lett. A **A** (1993) 244.
- [11] I.A.Bilenko, E.N.Ivanov, M.E.Tobar, D.G.Blair, Phys. Lett. A **211** (1996) 136.
- [12] V.B.Braginsky, V.P.Mitrofanov, K.V.Tokmakov, Phys. Lett. A **218** (1996) 164.

B. The effect of microdust particles on LIGO antenna (M.Gorodetsky)

Below I show that even one microdust particle placed in maximum of laser field in LIGO antenna may produce resonance shift comparable with that expected from gravitational wave.

Let a is the radius of a particle. I consider that this particle is placed near the center of the resonator of the length L and the square of the light spot on end mirrors is equal to $S = \pi D^2/4$. For simplicity I avoid analysis of the real configuration of the resonator and shall consider that the diameter D of the beam in the center is of the same order as on end mirrors. This approximation will make an estimate even more conservative.

In this case if $a \ll \lambda$ then the intensity of the scattered from this particle polarized light is described by the Rayleigh formula [1]

$$I = \frac{k^4 \alpha^2}{r^2} I_0 \sin^2 \theta \quad (79)$$

where $k = 2\pi/\lambda$ – is the wavenumber, r – is the distance from the particle, I_0 – is the intensity of the laser field of the mode of the resonator and θ is the angle between the mode polarization and the direction of scattering, and polarizability α for dielectrical particle is equal to

$$\alpha = \frac{(n^2 - 1)}{(n^2 + 2)} a^3 \quad (80)$$

(n is index of refraction) and in case of metal particle

$$\alpha = a^3 \quad (81)$$

This scattering leads to two different effects. The first and the simplest one is radiation losses (we shall characterise it with coefficient A^2). The second effect is connected with reflection of light from the particle back into the mode of the resonator (we shall characterise it with coefficient R^2). This effect is associated with a small fraction of light scattered with angles $|\pi - \theta| < D/L$ lying inside the mode caustic (I use here very simple estimates, more

rigorous approach with accurate account of overlap integrals and field distribution in LIGO interferometers may add more precise coefficients of the order of unity in all formulas). Another effect associated with phase shift of the light transmitted through the particle may be neglected if $na < \lambda$. After integrating (79) we obtain:

$$A^2 \simeq \frac{2\pi \int_0^\pi I r^2 \sin \theta d\theta}{I_0 S} = \frac{32k^4 \alpha^2}{3D^2} \quad (82)$$

and

$$R^2 \simeq \frac{SI(L/2, \pi)}{I_0 S} = \frac{4k^4 \alpha^2}{L^2} \quad (83)$$

It is interesting that reflection in our approximation does not depend on the diameter of the beam. The reason is simple : the larger is the diameter of the beam the less is scattering, but the larger part of the scattered light is caught by the mirrors and goes back to the mode.

Scattering particle inside the resonator should have the following transmittance matrix, satisfying conservation of energy:

$$S = \left\| \begin{array}{cc} Re^{i\phi \pm \pi/2} & T e^{i\phi} \\ T e^{i\phi} & Re^{i\phi \pm \pi/2} \end{array} \right\|, \quad (84)$$

where T – is transmittance, $T^2 + R^2 + A^2 = 1$, and ϕ is phaseshift. For very small particles it is evident to choose $\phi \simeq 0$. If this particle is placed at distance l from the left mirror then equations for internal amplitudes left and right to the particle will look as follows (I neglect here for simplicity transmittance losses in end mirrors):

$$\begin{cases} a_1 = T a_2 e^{2ik(L-l)} + i R a_1 e^{2ikl} \\ a_2 = T a_1 e^{2ikl} + i R a_2 e^{2ik(L-l)} \end{cases}, \quad (85)$$

Characteristic equation of this system

$$1 - (1 - A^2)e^{2ikL} - 2i R e^{ikL} \cos(2k(l - L/2)) \quad (86)$$

allows to determine additional frequency shift and additional losses produced by the particle as real and imaginary variations to k_0 , satisfying unperturbed equation $e^{2ik_0 L} = 1$.

$$\begin{aligned}
k' &= -\frac{R}{L} \cos(2k(l - L/2)) \\
k'' &= \frac{A^2}{L}
\end{aligned}
\tag{87}$$

In this way scattering leads to the broadening of the resonance (degradation of the quality factor).

$$\frac{\delta\omega}{\omega} = \frac{A^2}{kL} = \frac{32k^3\alpha^2}{3D^2L}
\tag{88}$$

and intermediate weak reflection leads to square averaged shift of the resonance frequency of the resonator:

$$\frac{\Delta\omega}{\omega} = \frac{R}{2kL} = \frac{k\alpha}{L^2}
\tag{89}$$

It is important that though $R^2 \ll A^2$, frequency shift is proportional to the first power of R and broadening is proportional to A^2 and for real parameters the second effect dominates.

Finally for dielectric particle with $n^2 = 2$ and $a = 3 \times 10^{-5} \text{ cm}$, using LIGO parameters $L = 4 \times 10^5 \text{ cm}$, $D = 10 \text{ cm}$ and $\lambda = 10^{-4} \text{ cm}$ I obtain

$$\frac{\Delta\omega}{\omega} = 3 \times 10^{-21}
\tag{90}$$

For metal particle this effect will be even 4 times larger. If this particle falls without initial speed from the ceiling of the tube, from the height of 50 cm then the time of perturbation while the particle crosses the beam will be $\sim 30 \text{ ms}$.

In other words only one dielectric microparticle with the radius of $1/3\lambda$ in 4 km resonator may simulate short 30 ms pulse of gravitational wave with $h = 3 \times 10^{-21}$.

If the size of the dust particle is much more than the wavelength formula (79) is not valid. In this case depending on material, form and surface of the particle scattering may be very complex. To estimate the effects, however one may use formulas for diffused scattering [1].

$$I = \frac{I_0 G f(\theta)}{4\pi r^2}
\tag{91}$$

where

$$f(\theta) = \frac{8}{2\pi}(\sin \theta - \theta \cos \theta) \quad (92)$$

and G is the mean geometrical crosssection of the particle. For convex bodies G is equal to one quarter of the square of the particle's surface so that for spherical particle evidently $G = \pi a^2$.

It is important that formula 91 is also valid for totally reflecting particles with smooth surface if we put $f(\theta) = 1$.

Finally as above we obtain very simple formulas for scattering and losses.

$$A^2 = f_1 \frac{4a^2}{D^2}, \quad (93)$$

and

$$R = f_2 \frac{a}{L}, \quad (94)$$

where f_1 and f_2 are coefficients of the order of unity depending on the form, smoothness, index of refraction of the particle. For white diffused spherical particle $f_2 = 4$.

Using the same parameters as above for a white particle with the radius $3\mu m$ we obtain:

$$\frac{\Delta\omega}{\omega} = 3 \times 10^{-19} \quad (95)$$

REFERENCES

- [1] H.C. van de Hulst, "Light scattering by small particles", New York, John Wiley & Sons, Inc., 1957.

C. The improvement of the Q -factors of the suspensions' modes and the search of the damping effect due to the electric field (V.Mitrofanov, N.Styazhkina, K.Tokmakov)

To achieve the highest possible quality factors for the suspensions' pendulum and violin modes the next step have been taken. The new vacuum chamber (where the tests of the pendulum and violin Q s are performed) was isolated from the rest of the room by a special box which permitted to reduce the level of the contamination of the fiber surface by dust approximately by one order. This box (which is supplied with the special dust free ventilation) also allows to fabricate the fibers for the suspension and to make the welding in the dust free environment as well as to install the pendulum in the chamber within few hours after the fabrication of the fibers. Two pendulums were fabricated during this half of year. Testing of the second one is now in progress. The preliminary results for this pendulum were obtained.

A 2-kg fused silica cylinder was suspended by two fused silica fibers with a length of about 25 cm and a diameter of about 0.2 mm. The fibers were welded to the small bumps which were carved in the cylinder and in the upper disk made from fused silica. The detail description of such suspension and the torsional-pendulum mode excited one can find in [1]. The resonant frequency of this mode was 0.31 Hz. The upper disk of this monolithic construction was rigidly attached to the cover of the vacuum chamber through the indium seals. The cover of the vacuum chamber was attached to a massive steel table rigidly fastened to the basic wall of the laboratory building. The chamber was pumped out by a turbomolecular pump. Residual gas pressure was less than 2×10^{-7} Torr. The excitation of the torsional-pendulum mode was performed by the special mechanical lever. The optical sensor was used to monitor the amplitude.

A plot of the pendulum amplitude as a function of time is shown in Fig. 3. The record begins within about 90 hours after excitation of the pendulum oscillation in order to exclude the influence of the transition process. Two interruptions of the record were at its end. The

full time of measurement was about 150 hours. The calculated magnitude of the relaxation time is about 1.5×10^8 seconds. Thus the measured Q of the torsional-pendulum mode is about 1.4×10^8 . This value is less than the Q expected from the theoretical analysis. The investigation of the weak dissipation mechanisms at this level of losses is now the main goal of the current researches.

The group continued the study of the electric field damping of the test mass oscillations. The experiments were carried out with a torsional pendulum made as a fused silica cylinder of radius 2.5cm and a mass of about 50g suspended by three welded fused silica fibers. The quality factor of the pendulum was $Q = 1.3 \times 10^7$. Conductive film was evaporated onto the bottom side of the cylinder. The electric field was applied between the bottom side of the pendulum and the electrode which was placed under the pendulum body. The electrode was made as a cylinder of radius 3cm with radial juts on the upper side and covered by the conductive film. The gap between the pendulum and the electrode was about 0.5mm. We checked noise in the power source electrical circuit to control the absence of electric discharges in the gap. The discharges were accompanied by surplus noise. The reason to choose this design of the pendulum was twofold. This made possible to apply high voltage with no change of pendulum spring constant. Thus, in the first place, the losses due to dissipation in the power source electrical circuit were eliminated, second, the dissipation caused by the electric field coupling between the pendulum and the electrode oscillations was minimized. The pendulum and the electrode were placed into the vacuum chamber.

The first experiments were carried out with aluminium covers of the electrode and the bottom side of the pendulum. The pendulum mode frequency was 1.25Hz. The electric field was found to cause an excess damping of the pendulum (Fig. 4). Heating in vacuum reduced the value of the excess losses approximately by factor two.

Further investigation was performed for the pendulum with resonant frequency of about 2.4Hz. The gold films were evaporated onto the electrode and pendulum surfaces. As in the case of aluminium covers, the excess damping was observed in the electric field. However, with the use of gold covers the value of the excess losses was significantly less than employing

aluminium ones (Fig. 4). This makes possible to conclude that the value of the excess losses are mainly determined by a material of the conductive covers. Thus surface processes supposedly may be responsible for the damping observed. This result has to be regarded as a preliminary one.

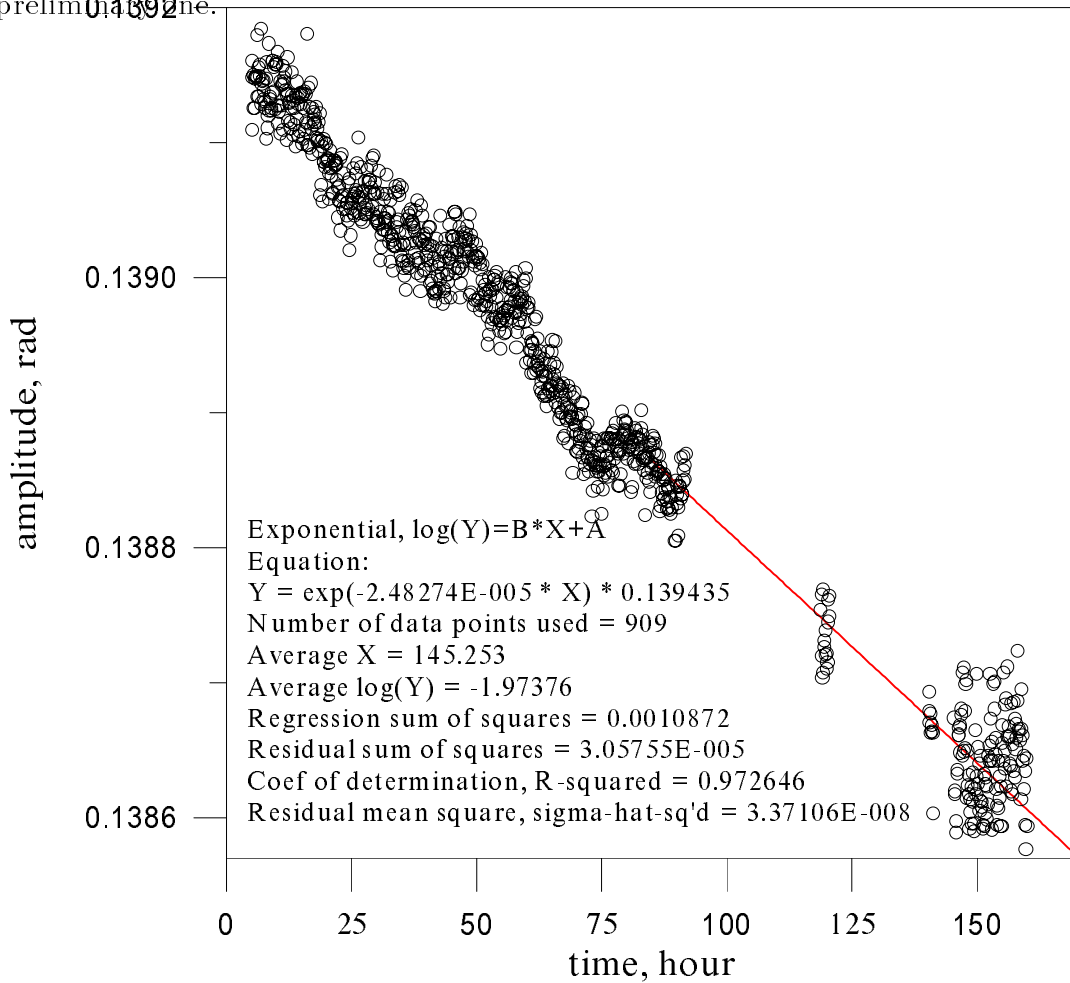


FIG. 3. Time dependence of the amplitude of the torsional-pendulum mode oscillations during a free decay.

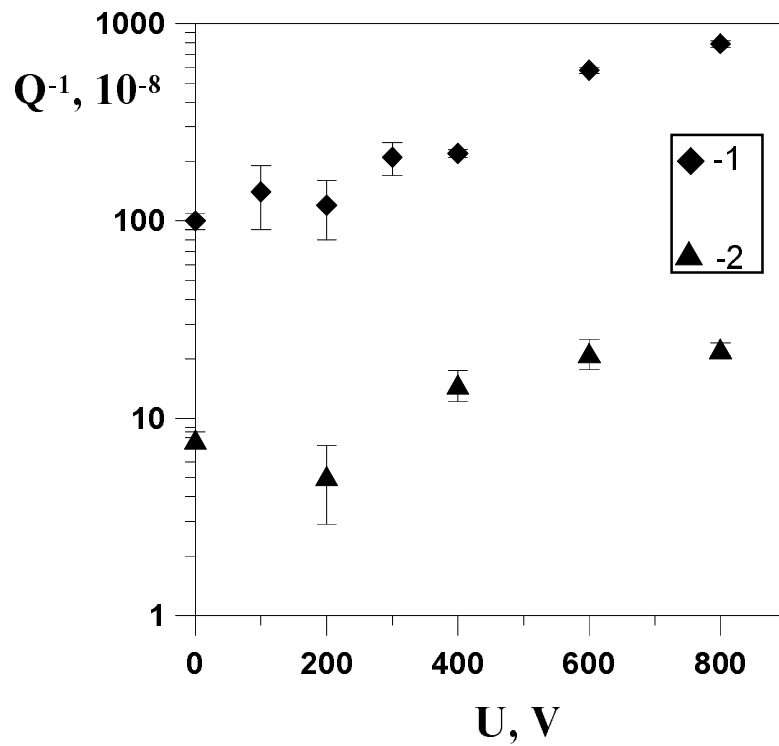


FIG. 4. Variation of Q^{-1} for the torsional pendulum as a function of the applied voltage U for 1-aluminium, 2-gold covers of the pendulum and the electrode surfaces.

REFERENCES

- [1] V.B.Braginsky, V.P.Mitrofanov and K.V.Tokmakov, Phys.Lett.A 218 (1996) 164.